Revisiting global vegetation controls using multi-layer soil moisture

Wantong Li[1*], Mirco Migliavacca[1], Matthias Forkel[2], Sophia Walther[1], Markus Reichstein[1] and René Orth[1]

[1]Department of Biogeochemical Integration, Max Planck Institute for Biogeochemistry, D-07745 Jena, Germany.

[2]Technische Universität Dresden, Institute of Photogrammetry and Remote Sensing, Helmholtzstr. 10, D-01069 Dresden, Germany.

*Corresponding author: Wantong Li (wantong@bgc-jena.mpg.de)

Key Points:

- Vertically resolved soil moisture improves the understanding of large-scale vegetation productivity.
- Extended water-related control on vegetation productivity emerges when considering multi-layer soil moisture versus total soil moisture.
- Sub-surface soil moisture is particularly important for vegetation productivity in semi-arid regions.

Abstract:

The productivity of terrestrial vegetation is determined by a multitude of drivers between the land surface and atmosphere. Water availability is critical for vegetation productivity, but the vertical dimension of soil moisture has been largely overlooked. Here, we analyze dominant controls of global vegetation productivity represented by sun-induced fluorescence and spectral vegetation indices at the half-monthly time scale. We apply random forests to predict anomalies of vegetation productivity from a comprehensive set of hydro-meteorological variables including multi-layer soil moisture and quantify the variable importance. Dominant hydro-meteorological controls generally vary with latitudes: temperature in higher latitudes, solar radiation in lower latitudes, and soil moisture from sub-surface layers in between. We find that including vertically resolved soil moisture allows a better understanding of vegetation productivity and reveals a broader water-related control. This is found especially for semiarid regions, illustrating the global relevance of deep(er) rooting systems as an adaptation to water limitation.

1. Introduction

Terrestrial vegetation is a key component coupling the global water and carbon cycles between the atmosphere and the land surface. Its productivity is determined by a multitude of hydro-meteorological variables (Monteith and Unsworth 1990; Nemani et al., 2003; Piao et al., 2020). While the underlying relationships are complex in time and space (Pearson et al., 2013; Cox et al., 2013; Garonna et al., 2018), the hydro-meteorological controls of anomalies in vegetation productivity are still not fully understood at a global scale. This knowledge gap contributes to uncertainties in assessing the sensitivity and resilience of ecosystems to different climate drivers (Seddon et al., 2016; Sakschewski et al., 2016), and in future climate projections (Feng et al., 2014; Novick et al., 2016; Duveiller et al., 2018).

Previous studies investigated dominant hydro-meteorological controls of vegetation productivity at a global scale and across different ecosystems (Nemani et al., 2003; Beer et al. 2010; Jung et al. 2011; Seddon et al., 2016; Madani et al., 2017; Jung et al., 2017; Walther et al., 2019; Li & Xiao, 2020). While these studies and recent gross primary production (GPP) estimates agree that vegetation in (semi-)arid area is significantly impacted by soil moisture (SM) (Stocker et al., 2018; Stocker et al., 2020), a corresponding global analysis including the impact

of SM from multiple depths is lacking. Several studies have already highlighted the local relevance of multi-layer SM to ecosystems: root water uptake from deeper soil layers can help mitigate water stress and maintain plant transpiration (Schulze et al., 1996; Migliavacca et al., 2009); A et al., 2019 demonstrated varying relative importance of surface SM versus deeper SM depending on land cover types; and Schlaepfer et al., 2017 simulated an increased dryness of sub-surface SM compared to surface SM which largely impacted vegetation dynamics in temperate drylands. This way, distinguishing shallow and deep SM is expected to allow for a more accurate identification of global vegetation controls as the accessibility and availability of water for plants varies in space and time. For this purpose, the state-of-the-art ERA5 reanalysis provides SM estimates from multiple layers (Hersbach et al. 2019; Jing et al., 2018), and has been successfully applied in hydro-meteorological studies (Jing et al., 2018; Tarek et al., 2020; Li et al., 2020).

When considering multiple hydro-meteorological variables, the identification of global vegetation controls is challenged by potential high collinearity (Dormann et al., 2013) between some of the variables. Most previous studies did not consider more than three variables, thereby somewhat circumventing this problem while ignoring potentially important variables (Seddon et al., 2016; Garonna et al., 2018; Claessen et al., 2019; Li & Xiao, 2020). Machine learning methods such as random forests have no assumptions on the input data characteristics, and are designed to process large amounts of diverse input data (Breiman 2001; Forkel et al. 2019; Jiao et al. 2019). Though they are also challenged by the collinearity in the input data, they are better placed to deal with this than traditional statistical methods. Further, a pre-processing of the data can mitigate collinearity by removing potential confounding signals such as long-term trends or the seasonality (Jung et al., 2017).

Aside from model-based estimates (e.g. Jung et al. 2020), reliable observation-based global photosynthesis proxies are only available for recent years through satellite-derived sun-induced fluorescence (SIF, Baker et al., 2008; Frankenberg et al., 2011; Joiner et al.,2013). SIF data is increasingly used to study the relationships between global vegetation productivity and hydro-meteorological drivers (Yang et al., 2015; Ying et al., 2015; Wagle et al., 2016; Zuromski et al., 2018; Jiao et al., 2019; Walther et al., 2019; Li & Xiao, 2020). Besides, spectral vegetation indices and biophysical parameters from multi-spectral satellite instruments such as the Moderate Resolution Imaging Spectroradiometer (MODIS) are widely used to study drivers

of vegetation phenology and productivity (Forkel et al. 2015; Seddon et al., 2016; Buermann et al., 2018). In this study, we consider SIF alongside two spectral indices (the normalized difference vegetation index, NDVI; and near-infrared reflectance of terrestrial vegetation, NIRv), and a comprehensive set of explanatory variables representing energy (temperature; radiation; vapor pressure deficit, VPD) and water availability (precipitation; multi-layer SM) to revisit global photosynthesis and greenness controls.

2. Data and Methods

2.1. Vegetation Target Data

2.1.1. Sun-Induced Fluorescence (SIF)

SIF is a proxy for photosynthesis as it captures radiation emitted by chlorophyll molecules and is related to photosynthetic activity. We use one of the longest available satellite-derived SIF retrieval which is based on the Global Ozone Monitoring Experiment–2 (GOME-2) instrument and ranges from 2007 to 2018 (Köhler et al., 2015). The raw global SIF observations are filtered to remove data based on (i) high solar zenith angles (>70˚), (ii) large differences to the normal local overpass time (2 p.m-8 a.m in the next day), and (iii) large cloud cover (>50%), as done by Köhler et al., 2015.

2.1.2. Vegetation Indices

To complement the photosynthesis analysis we use NDVI and NIRv as spectral vegetation indices (Huete et al., 2002; Badgley et al., 2017). We obtain red and near-infrared reflectances from MOD13C1 v006 product (https://lpdaac.usgs.gov/products/mod13c1v006/) in an original 16-day and 0.05˚ resolution. NDVI and NIRv are computed from data with quality flags 0 and 1.

2.2. Hydro-meteorological predictor data

We consider a comprehensive selection of energy and water-related variables from the ERA5 reanalysis (Hersbach et al., 2019). Energy-related variables include air temperature at 2-m height (hereafter referred to as temperature), surface downward solar radiation (solar radiation) and VPD, and the water-related variables are total precipitation (precipitation), SM layer 1 (0-7

cm), layer 2 (7-28 cm), layer 3 (28-100 cm) and layer 4 (100-289 cm). For comparison, we compute total SM by averaging values across the individual layers weighted by their thickness. It is to note that VPD is related to the relative humidity and temperature, and hence we treat it as an energy-related variable, while it represents the demand of the water in the atmosphere.

To validate our findings we also use alternative SM products: (i) MERRA-2 surface and root-zone SM (Gelaro et al., 2017), (ii) GLEAM v3.3 surface and root-zone SM (Martens et al., 2017), and (iii) SoMo.ml with three layers (O and Orth, 2020). Table S1 shows the information of depths for all SM products that we use and classify into surface SM, shallow and deep root-zone SM.

2.3. Additional data

To evaluate the results of our analyses, we compute the aridity index for each grid cell as the ratio between the long-term averages of net radiation (expressed as mm potential evaporation) and precipitation from the respective ERA5 data. We distinguish climate regimes using long-term mean temperatures and aridity index. In addition, we use fractional vegetation coverage (FVC) data from the AVHRR vegetation continuous fields products (VCF5KYR, https://lpdaac.usgs.gov/products/vcf5kyrv001/) from 2007 to 2016 to classify the percentages of tree canopy, short vegetation and bare ground (Song et al., 2018). We distinguish vegetation characteristics using the fraction of vegetation cover (the sum of the fractions of tree canopy and short vegetation), and the fraction of tree cover in vegetation cover.

2.4. Methods

2.4.1. Data Pre-processing

The data pre-processing is illustrated in Figure S1. All vegetation indices and hydro-meteorological data are aggregated to 0.5° spatial and half-monthly temporal resolution where SIF is available, and 16-day original NDVI and NIRv are linearly interpolated to half-monthly resolution. The study time period is 2007-2018, limited by the availability of SIF. In all SIF-based analyses we focus on data with SIF > 0.5 $mW/m^2/sr/nm$ to filter out sparse or dormant vegetation. This filtering is also applied in the NDVI and NIRv analyses, where additionally negative NDVI and NIRv values are filtered out. Grid cells are only considered in the analysis if more than 15 data points are left after filtering, and if the vegetation cover from the FVC data exceeds 5%. For all target and predictor variables, we obtain half-monthly anomalies by

subtracting the mean seasonal cycles. We remove long-term trends for each grid cell which are determined by a locally weighted smoothing filter (Cleveland et al., 1979) with a smoothing span of 0.4.

2.4.2. Identification of main controls

Random forests (RF) is a non-parametric regression-based method requiring no statistical assumptions on predictor and target variables (Breiman 2001). In this study, all hydro-meteorological anomalies are used as predictor variables, and anomalies of SIF and vegetation indices are employed as target variables per each grid cell, respectively (Figure S1). RF training is done using information from each grid cell together with the surrounding grid cells (forming 3x3 grid cell matrices) to yield robust model performance while including data with similar climatic and landscape characteristics. After training, the performance of the RF model is evaluated at each grid cell by computing the R^2 between the modeled and observed target variable for out-of-bag (OOB) data that was not used for training (hereafter referred as R^2). Grid cells with R^2 lower than or equal to 0 are filtered out.

The relative importance of each predictor variable is inferred from the decrease in R^2 related to a temporal permutation applied to the particular variable (Cutler et al., 2012; Gómez-Ramírez et al., 2019). To validate our findings we additionally employ two more methods in this context: (i) Spearman correlation between each predictor variable and SIF, NDVI or NIRv (Zwillinger & Kokoska, 2000) and (ii) SHapley Additive exPlanations (SHAP) feature importance which is based on the average marginal contribution of each predictor to the modeled target variable (Lundberg et al. 2017; Sundararajan et al., 2019).

In addition to the determination of the most relevant hydro-meteorological controls we study the sensitivity of the vegetation response to each predictor variable. The sensitivity is determined by the slope from fitted linear quantile (median) regression between the SHAP dependence of a target variable and a predictor variable, as SHAP dependence enables to measure the marginal effect each predictor variable has on the target variable for individual and global explanations (Lundberg et al. 2017; Forkel et al., 2019). While the magnitude of the sensitivity is usually similar to the identification of feature importance, the sign of sensitivity complements the information in importance identification. All data-processing and analyses are done with Python 3.7 by using the NumPy 1.16.1 (Oliphant 2006), Statsmodels 0.11.1 (Skipper

& Perktold, 2010), Scikit-learn 0.22.1 (Pedregosa et al., 2011), Matplotlib (Hunter 2007) and shap 0.35.0 packages (Lundberg et al. 2017).

3. Results and Discussion

3.1. Model performance

Two experiments are performed with RF models differing in how SM is accounted for (i.e. total versus multi-layer SM), while precipitation, VPD, solar radiation, and temperature are used consistently in both experiments. Results show that the performance of the RF model in predicting SIF anomalies is higher using multi-layer SM than that with total SM (Figure 1).

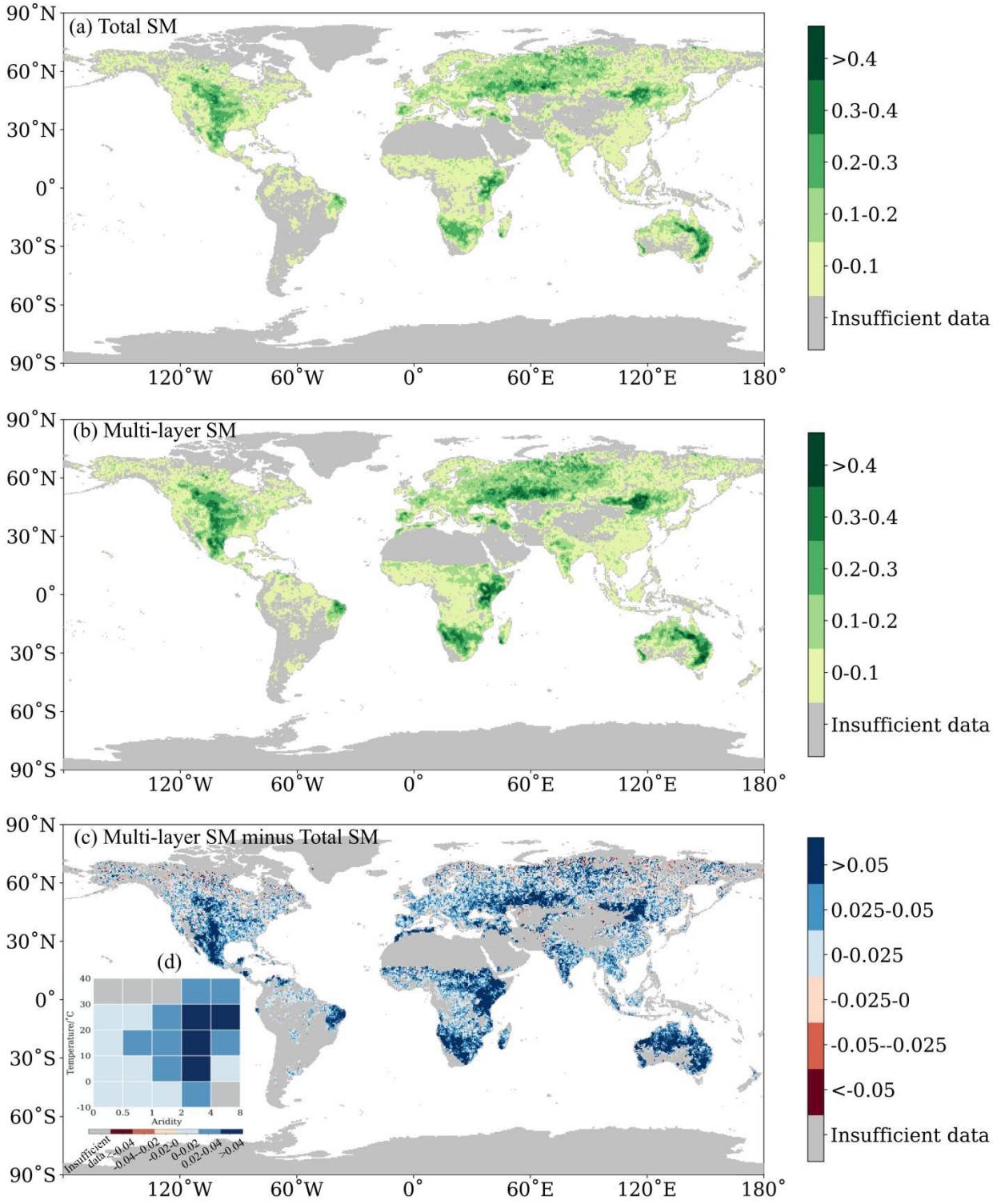

Figure 1. Model performance (R^2) in predicting Sun-Induced Fluorescence (SIF) in (a) the total soil moisture (SM) experiment and (b) the multi-layer SM experiment (SM layers 1-4). The panel (c) is the difference between (b) and (a), and (d) summarizes their differences across climate regimes (i.e. Temperature and Aridity).

The spatial patterns of model performance are similar between both experiments with higher R2 (> 0.3) in the central North America, central Eurasia, southern and eastern Africa, central Asia, and eastern Australia. The predictive performance is improved in most regions across the globe when using multi-layer instead of total SM. Improvements are particularly found in semi-arid regions such as Australia, central North America and central Asia (Figure 1c, d). Since multi-layer SM may experience different dynamics across time and space (Schlaepfer et al., 2017; Berg et al., 2016; Zhang et al., 2016; Lian et al., 2020), plant rooting systems can develop to adapt for localized water deficits (Fan et al., 2017), such that vertical SM information can be especially useful in semi-arid regions to predict the vegetation productivity.

Though the performance of SIF prediction is improved with multi-layer SM, the R^2 values are still relatively low in many regions. There are even some regions that show R^2 lower than 0 in South America and central Australia, indicating a worse model performance than a constant mean value prediction. Such limited reliability of SIF predictions may relate to the noise of satellite-derived SIF, for example, large regions in South America are located near to the known South Atlantic Anomaly, which disturbs the satellite-based SIF retrievals (Joiner et al., 2013; Köhler et al., 2015). This disturbance is less relevant for the NDVI and NIRv retrievals such that RF model performance is better (Figure S2). Despite the weak model performance in the case of SIF we believe that our methodology is robust to infer main hydro-meteorological controls of vegetation productivity, because (i) the employed R^2 of out-of-bag anomaly data is a challenging metric where information cannot be derived from e.g. seasonal variations or trends, and also other studies found similarly low values (Kraft et al., 2019); and (ii) main hydro-meteorological controls on SIF anomalies identified by RF model resemble global patterns reported in previous studies about main climatic drivers to absolute variations of vegetation productivity (Figure 2) (Nemani et al., 2003; Seddon et al., 2016; Madani et al., 2017).

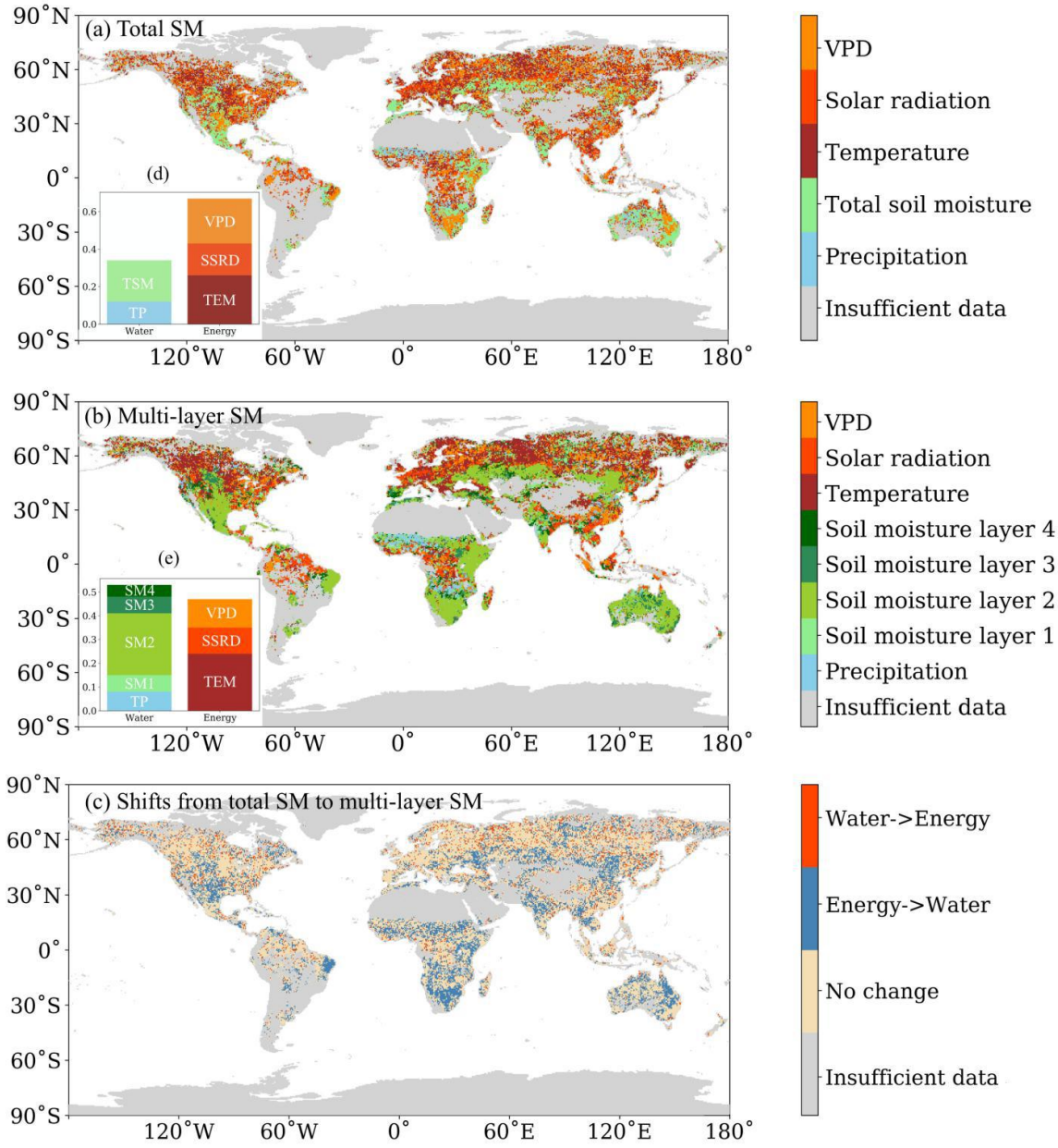

207

208 **Figure 2. Main hydro-meteorological controls on sun-induced fluorescence (SIF) by applying (a)**
209 **total soil moisture (SM) alongside all other predictor variables, and (b) multi-layer SM alongside**
210 **all other predictor variables. (c) Shifts between the energy and water controls from (a) to (b).**
211 **Proportions of global land area where each variable is the most important controlling factor are**
212 **shown in (d) and (e). In (d) and (e), TP denotes precipitation; TSM denotes total soil moisture;**
213 **SM1, 2, 3, 4 denote soil moisture in layers 1, 2, 3, 4 respectively; TEM denotes temperature; SSRD**
214 **denotes solar radiation; And VPD denotes vapor pressure deficit. As shown in Table S1, SM layer**
215 **1 in ERA5 belongs to surface SM, SM layer 2 and 3 belong to shallow root-zone SM, and SM layer**
216 **4 belongs to deep root-zone SM.**

We perform further RF model experiments to investigate if the added skill in the case of the multi-layer SM is related to the increased number of predictor variables, and therefore an increased flexibility of the model, or to the additional information contained in the individual layers compared with the total SM. First, the experiment of multi-layer RF (4 variables) preforms better than the experiment of 5 SM variables, showing that the enhanced performance is not exclusively due to the increased number of variables and related to increased flexibility of the RF model (Figure S3). Second, regionally enhanced performance can be found when replacing total SM with individual layers (Figure S4), indicating that additional information can be explored by the RF model from SM from individual layers.

3.2. Main hydro-meteorological controls on global vegetation productivity

The global patterns of main SIF controls are clearly different between the analyses with total SM and with multi-layer SM (Figure 2); Total SM does not provide sufficient information to the RF model to detect all water-controlled regions while these regions are actually covering the majority of the Earth's land in the analysis with multi-layer SM. Overall, temperature is identified as the main driver of SIF in the higher northern latitudes, solar radiation dominantly controls SIF in most tropical regions, and VPD emerges as a main control on SIF in parts of the western Amazon forests, eastern North America, northern Eurasia and eastern Asia. In between the tropics and the higher latitudes, where mostly semi-arid climate regimes are prevailing, water-related variables play the dominant role in controlling SIF. Precipitation and surface SM control SIF in central India, western Sahel and transition regions between central and southern Africa. Root-zone SM mainly controls SIF in southern North America, southern Europe, and many parts of Eurasia, India and Australia. In general, shallow-root zone SM emerges as the most relevant SM reservoir for vegetation productivity, while deeper SM is particularly important in the transitional zones and temperate dry regions, such as central North America and southern South Europe.

Key drivers of NIRv and NDVI present similar global patterns to those of SIF (Figure S5), while they show extended SM-controlled regions. Walther et al., 2019 also found inconsistent values of tree cover fraction with shifting relationships between SM and SIF or vegetation indices, relating to the fact that spectral greenness signals are somewhat influenced by moisture-related changes in the soil reflectivity or plant water content. Further, for the

247 respective main controlling hydro-meteorological variables identified across space, we typically
248 find highly positive associated sensitivities of SIF to the respective control, which supports
249 positive relationships between the identified main controls and SIF (Figure S6).
250 Next, we analyze the main controls with respect to climate regimes. Figure 3a shows that
251 the SM variables dominantly control SIF in arid regions, energy-related variables dominantly
252 control SIF in humid regions. In transitional regions water-related variables tend to be more
253 important at warmer temperatures, while energy-related variables dominate for colder
254 temperatures. Overall, the pattern is in line with first-order constraints for evapotranspiration
255 from Seneviratne et al., 2010, and with findings on energy- versus water-dominated vegetation
256 by Denissen et al. 2020 in Europe. Across all considered hydro-meteorological variables,
257 shallow-root zone SM is identified as the most important variable in (semi-)arid regions. Among
258 the energy variables temperature is the most relevant, while solar radiation also plays a role
259 particularly in warm regions. Similar patterns are found for NDVI and NIRv with SM controls
260 extending more beyond arid regions (Figure 3b, c).
261

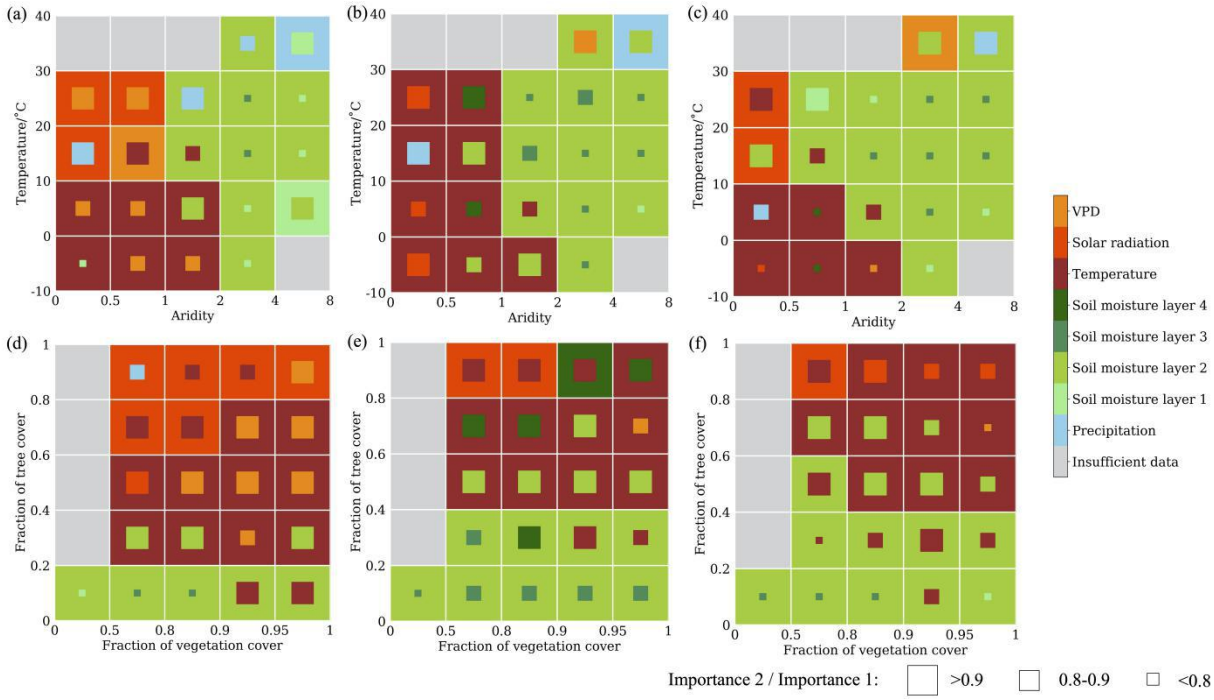

Figure 3. Main hydro-meteorological controls on (a, d) sun-induced fluorescence SIF, (b, e) Near-Infrared reflectance vegetation indices (NIRv) and (c, f) normalized difference vegetation indices (NDVI) across climate regimes and vegetation characteristics. Most important control variables are indicated by the color of the temperature-aridity and tree-vegetation boxes, respective second most important control variables are denoted by the color of the inner square, where the size indicates the relative importance compared to the most important control variable. Temperature-aridity and tree-vegetation boxes containing less than 10 available data are shown in gray. The aridity index and the fraction of vegetation cover are visualized by non-linear sequences in terms of skewed distributions of the data.

Main controls also differ with vegetation types (Figure 3d, e, f), mostly varying along a gradient in the fraction of tree cover while they are more similar between different fractions of vegetation cover. Regions dominated by grass or shrubs are most water-controlled, regions with intermediate tree cover are temperature-controlled, and regions with the highest tree cover and presumably wet or temperate climate conditions are mostly radiation-controlled. Such main energy controls involve a relatively lower vulnerability of tree ecosystems to droughts than other ecosystems (Huang & Xia, 2019), as droughts are typically associated with above-average solar

radiation and newly developing leaves that can compensate photosynthesis (Orth & Destouni, 2018; Yan et al., 2019; Hutyra et al., 2007; Wu et al., 2016; Li et al., 2018b). Moreover, consistent with the previous findings, NDVI and NIRv show extended significant water-related controls to tree-grass mixed biomes compared with the SIF results (Walther et al., 2019). This is more pronounced for NDVI, potentially due to larger confounding effects of background brightness in NDVI, while NIRv contains enhanced information about the proportion of vegetation in reflectance and partly overcomes this issue (Badgley et al., 2017; Badgley et al., 2019). Changes in main controls across vegetation characteristics are not simply an artifact of the correspondingly different climate regimes, as Figure S7 shows that the main hydro-meteorological controls change in response to both vegetation type and climate.

3.3. Main water-related controls on global vegetation productivity

Focusing exclusively on water-related controls reveals that the most important soil layer varies across climate and vegetation characteristics (Figure 4). Shallow-root zone SM is most relevant in semi-arid conditions and for grass or shrubs, indicating that plants can adapt to water-scarce conditions at the surface with deeper-reaching rooting systems (Fan et al., 2017). This is in line with previous but smaller-scale studies: A et al., 2019 found the strongest relationship between evapotranspiration and SM between 10-100 cm depth for site-scale experiments in a transitional zone; further, in dry surface soils in (semi-)arid regions, plants could easily alter rooting depth distribution and root morphology to utilize water from deeper soil layers (Schulze et al., 1996), for instance in local Mediterranean grass (Barkaoui et al., 2016) or savannas ecosystems (Hoekstra et al., 2014; Nippert & Holdo, 2015). For even drier climate conditions, shallower soil layers become more relevant, probably because the low water supply does not sustain the development of deep(er) rooting systems such that intermittent vegetation growth mostly benefits from rainfed surface SM. Interestingly, towards humid climate conditions our analysis shows a dominant role of surface SM and precipitation, while at the same time these regions are characterized by high tree cover with deep roots. This could be due to frequent precipitation keeping surface soil layers wet such that plants can extract significant fractions of their water demand from there, while the dependence on deeper layers for trees during short drought periods is not reflected. Furthermore, we note that these regions are controlled by temperature or solar radiation (see Figure 3) such that the results here could also

be an artifact as precipitation and partly also surface SM are expected to co-vary more strongly with the dominant energy variables than deeper-layer SM.

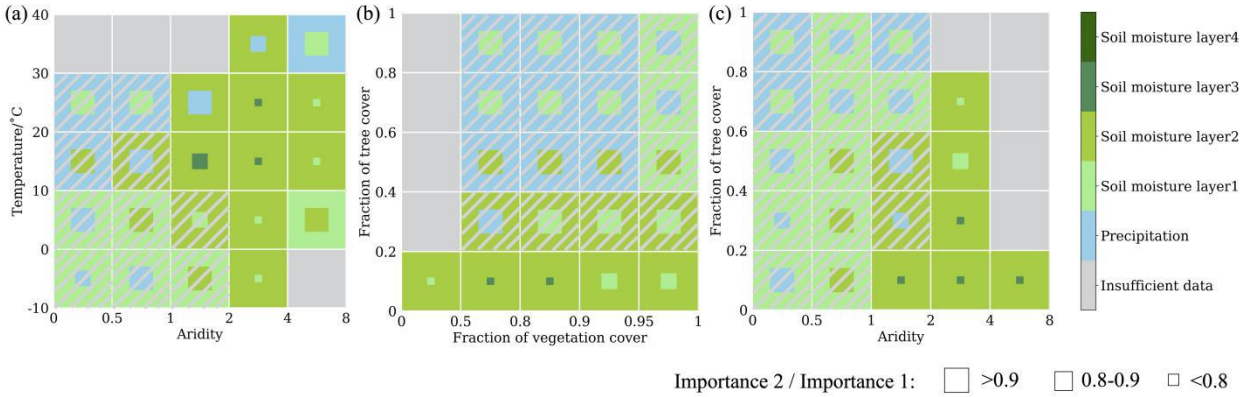

Figure 4. Main water-related controls on sun-induced fluorescence (SIF) across (a) climate regimes, (b) vegetation characteristics, and (c) classes of fraction of tree covers and aridity. Similar to Figure 3 but focusing on SIF and water-related controls only. The gray hatching indicates that temperature, solar radiation or VPD are identified as main controls on SIF in these boxes in Figure 3.

To illustrate the robustness of our results, we repeat the previous analyses with different setups: (i) we use Spearman correlation (Figure S8) and SHAP feature importance (Figure S9) as alternative ways to estimate the importance of the considered predictor variables for SIF dynamics, and find similar results as for the permutation importance approach, and (ii) we use alternative SM products, namely GLEAM, MERRA-2 and SoMo.ml (Figure S10), all of which lead to similar results as found with the ERA5 SM.

We acknowledge, however, that our analyses do not consider seasonal compensation effects, memory effects and irrigation effects when illustrating main hydro-meteorological controls on vegetation productivity. Memory effects are found occurring particularly in transitional water-driven biomes and sub-tropical regions (Kraft et al., 2019). Precipitation from wet seasons can serve as subsurface water storage in subsequent dry seasons (Guan et al., 2015), and water transport in roots and stems might be slow or delayed for tree ecosystems, affecting energy- or water-control characteristics across biomes. Besides, warm springs benefit photosynthesis in the early stage of the growing season, while induce water deficits in the later seasons in northern energy-limited ecosystems (Buermann et al., 2018). Finally the main hydro-meteorological controls which we determine for the entire growing season may vary between the

335 early, mid and later parts of this period. We further note that our analyses is based on specific
336 spatial and temporal scales, while vegetation-climate relationships can differ between short-term
337 and long-term scales (Linscheid et al., 2019), and contrasting signals from nearby regions could
338 lead to inconclusive results (Jung et al., 2017).
339

4. Conclusions

This study illustrates that the information of vertically resolved SM improves the understanding and modeling of anomalies of vegetation productivity. Thereby, vegetation relies on water from different depths while these characteristic depths vary with climate and vegetation type. In particular, we show at the global scale that vegetation in semi-arid regions is adapted to dry conditions through deep(er) rooting systems ensuring more continuous water supply from deeper soil layers. This complexity was not sufficiently acknowledged in previous studies; future research should account for vertical SM dynamics by considering multiple layers. The development of hydrology, land surface, and vegetation models should focus on a reliable representation of soil layers and vertical soil water transport.

Further, we compare the hydro-meteorological controls of vegetation productivity obtained with different respective proxy metrics. SIF is more strongly related to photosynthesis, and eventually the carbon cycle, compared with NDVI and NIRv, but SIF data is only available for recent years. Our results show that NDVI and NIRv, which are available from the early 1980s, yield similar patterns except for a consistent overestimation of water controls, probably induced by changes of soil background reflectance as a response to soil moisture changes.

Overall, our study contributes to advanced process of understanding within the role of soil moisture on vegetation productivity by benefiting from the ever-growing suite of global eco-hydrological data streams.

Acknowledgments

The authors declare no conflict of interest. We thank Ulrich Weber for processing hydro-meteorological data and MODIS data. W. L., R. O., and M. M. acknowledge the financial support of the China Scholarship Council that funded the PhD scholarship of W.L. W. L. also acknowledges this work under the International Max Planck Research School for Global Biogeochemical Cycles. R. O. was funded by the German Research Foundation (Emmy Noether grant number 391059971), and S. W. acknowledges funding by an ESA Living Planet Fellowship 'Vad3e mecum'. SIF GFZ data have been retrieved from ftp://fluo.gps.caltech.edu/data/Philipp/GOME-2/ungridded/. ERA5 data can be downloaded from https://cds.climate.copernicus.eu/, GLEAM SM from https://www.gleam.eu/, MERRA-2 SM data from https://gmao.gsfc.nasa.gov/reanalysis/MERRA-2/FAQ/, and SoMo.ml from ftp://ftp.bgc-jena.mpg.de/pub/outgoing/sungmino/somo_v1/. All the links of the data are accessed on 29 September 2020.

References

A, Y., Wang, G., Liu, T., Xue, B., & Kuczera, G. (2019). Spatial variation of correlations between vertical soil water and evapotranspiration and their controlling factors in a semi-arid region. *Journal of Hydrology*, *574*, 53-63. https://doi.org/10.1016/j.jhydrol.2019.04.023

Albergel, C., Dorigo, W., Reichle, R., Balsamo, G., De Rosnay, P., Muñoz-Sabater, J., Isaksen, L., De Jeu, R., & Wagner, W. (2013). Skill and global trend analysis of soil moisture from reanalyses and microwave remote sensing. *Journal of Hydrometeorology*, *14*(4), 1259-1277. https://doi.org/10.1175/JHM-D-12-0161.1

Badgley, G., Field, C. B., & Berry, J. A. (2017). Canopy near-infrared reflectance and terrestrial photosynthesis. *Science Advances, 3*(3), e1602244. https://doi.org/10.1126/sciadv.1602244

Badgley, G., Anderegg, L. D. L., Berry, J. A., & Field, C. B. (2019). Terrestrial gross primary production: Using NIRV to scale from site to globe. *Global Change Biology*, *25*(11), 3731-3740. https://doi.org/10.1111/gcb.14729

Baker, N. R. (2008). Chlorophyll fluorescence: a probe of photosynthesis in vivo. *Annual Review of Plant Biology*, *59*, 89-113. https://doi.org/10.1146/annurev.arplant.59.032607.092759

Barkaoui, K., Roumet, C., & Volaire, F. (2016). Mean root trait more than root trait diversity determines drought resilience in native and cultivated Mediterranean grass mixtures. *Agriculture, Ecosystems & Environment*, *231*, 122-132. https://doi.org/10.1016/j.agee.2016.06.035

Beer, C., Reichstein, M., Tomelleri, E., Ciais, P., Jung, M., Carvalhais, N., ... & Papale, D. (2010). Terrestrial gross carbon dioxide uptake: global distribution and covariation with climate. *Science, 329*(5993), 834-838. https://doi.org/10.1126/science.1184984

Berg, A., Sheffield, J., & Milly, P. C. (2017). Divergent surface and total soil moisture projections under global warming. *Geophysical Research Letters*, *44*(1), 236-244. https://doi.org/10.1002/2016GL071921

Breiman, L. (2001). Random forests. Mach. Learning 45, 5–32.

Buermann, W., Forkel, M., O'Sullivan, M., Sitch, S., Friedlingstein, P., Haverd, V., Jain, A. K., Kato, E., Kautz, M., & Lienert, S. (2018). Widespread seasonal compensation effects of spring warming on northern plant productivity. *Nature*, *562*(7725), 110-114. https://doi.org/10.1038/s41586-018-0555-7

Claessen, J., Molini, A., Martens, B., Detto, M., Demuzere, M., & Miralles, D. (2019). Global biosphere-climate interaction: a causal appraisal of observations and models over multiple temporal scales. *Biogeosciences*, *16*(24), 4851-4874. https://doi.org/10.5194/bg-16-4851-2019

Cleveland, W. S. (1979). Robust locally weighted regression and smoothing scatterplots. *Journal of the American Statistical Association*, 74(368), 829-836. https://doi.org/10.1080/01621459.1979.10481038

Cox, P. M., Pearson, D., Booth, B. B., Friedlingstein, P., Huntingford, C., Jones, C. D., & Luke, C. M. (2013). Sensitivity of tropical carbon to climate change constrained by carbon dioxide variability. *Nature*, *494*(7437), 341-344. https://doi.org/10.1038/nature11882

Cutler A., Cutler D.R., & Stevens J.R. (2012) Random Forests. In: Zhang C., & Ma Y. (eds) Ensemble Machine Learning. Springer, Boston, MA. https://doi.org/10.1007/978-1-4419-9326-7_5

Denissen, J. M., Teuling, A. J., Reichstein, M., & Orth, R. (2020). Critical soil moisture derived from satellite observations over Europe. *J. Geophys. Res. Atmos.*, e2019JD031672. https://doi.org/10.1029/2019JD031672

Dormann, C. F., Elith, J., Bacher, S., Buchmann, C., Carl, G., Carré, G., Marquéz, J. R. G., Gruber, B., Lafourcade, B., & Leitao, P. J. (2013). Collinearity: a review of methods to deal with it and a simulation study evaluating their performance. *Ecography*, *36*(1), 27-46. https://doi.org/10.1111/j.1600-0587.2012.07348.x

Duveiller, G., Hooker, J., & Cescatti, A. (2018). The mark of vegetation change on Earth's surface energy balance. *Nature Communications*, *9*, 679. https://doi.org/10.1038/s41467-017-02810-8

Fan, Y., Miguez-Macho, G., Jobbagy, E. G., Jackson, R. B., & Otero-Casal, C. (2017). Hydrologic regulation of plant rooting depth. *Proceedings of the National Academy of Sciences*, *114*(40), 10572-10577. https://doi.org/10.1073/pnas.1712381114

Feng, S., Hu, Q., Huang, W., Ho, C.-H., Li, R., & Tang, Z. (2014). Projected climate regime shift under future global warming from multi-model, multi-scenario CMIP5 simulations. *Global and Planetary Change*, *112*, 41-52. https://doi.org/10.1016/j.gloplacha.2013.11.002

Forkel, M., Migliavacca, M., Thonicke, K., Reichstein, M., Schaphoff, S., Weber, U., & Carvalhais, N. (2015). Codominant water control on global interannual variability and trends

in land surface phenology and greenness. *Global Change Biology*, *21*(9), 3414-3435. https://doi.org/10.1111/gcb.12950

Forkel, M., Andela, N., Harrison, S. P., Lasslop, G., van Marle, M., Chuvieco, E., Dorigo, W., Forrest, M., Hantson, S., Heil, A., Li, F., Melton, J., Sitch, S., Yue, C., & Arneth, A. (2019). Emergent relationships with respect to burned area in global satellite observations and fire-enabled vegetation models. *Biogeosciences*, *16*(1), 57-76. https://doi.org/10.5194/bg-16-57-2019

Frankenberg, C., Fisher, J. B., Worden, J., Badgley, G., Saatchi, S. S., Lee, J. E., Toon, G. C., Butz, A., Jung, M., & Kuze, A. (2011). New global observations of the terrestrial carbon cycle from GOSAT: Patterns of plant fluorescence with gross primary productivity. *Geophysical Research Letters*, *38*, L17706. https://doi.org/10.1029/2011gl048738

Frankenberg, C., O'Dell, C., Berry, J., Guanter, L., Joiner, J., Köhler, P., Pollock, R., & Taylor, T. E. (2014). Prospects for chlorophyll fluorescence remote sensing from the Orbiting Carbon Observatory-2. *Remote Sensing of Environment*, *147*, 1-12. https://doi.org/10.1016/j.rse.2014.02.007

Garonna, I., de Jong, R., Stöckli, R., Schmid, B., Schenkel, D., Schimel, D., & Schaepman, M. E. (2018). Shifting relative importance of climatic constraints on land surface phenology. *Environmental Research Letters*, *13*(2), 024025. https://doi.org/10.1088/1748-9326/aaa17b

Gelaro, R., McCarty, W., Suárez, M. J., Todling, R., Molod, A., Takacs, L., Randles, C. A., Darmenov, A., Bosilovich, M. G., & Reichle, R. (2017). The modern-era retrospective analysis for research and applications, version 2 (MERRA-2). *Journal of Climate*, *30*(14), 5419-5454. https://doi.org/10.1175/JCLI-D-16-0758.1

Gómez-Ramírez, J., Ávila-Villanueva, M., & Fernández-Blázquez, M. Á. (2019). Selecting the most important self-assessed features for predicting conversion to Mild Cognitive Impairment with Random Forest and Permutation-based methods. *bioRxiv*, 785519. https://doi.org/10.1101/785519

Guan, K., Pan, M., Li, H., Wolf, A., Wu, J., Medvigy, D., Caylor, K. K., Sheffield, J., Wood, E. F., Malhi, Y., Liang, M., Kimball, J. S., Saleska, Scott R., Berry, J., Joiner, J., & Lyapustin, A. I. (2015). Photosynthetic seasonality of global tropical forests constrained by hydroclimate. *Nature Geoscience*, *8*(4), 284-289. https://doi.org/10.1038/ngeo2382

Hersbach, H., Bell, B., Berrisford, P., Horányi, A., Sabater, J. M., Nicolas, J., Radu, R., Schepers, D., Simmons, A., & Soci, C. (2019). Global reanalysis: goodbye ERA-Interim, hello ERA5. *ECMWF newsletter*, *159*, 17-24. https://doi.org/10.21957/vf291hehd7

Hoekstra, N. J., Finn, J. A., Hofer, D., & Lüscher, A. (2014). The effect of drought and interspecific interactions on depth of water uptake in deep-and shallow-rooting grassland species as determined by δ^{18} O natural abundance. *Biogeosciences*, *11*(16), 4493-4506. https://doi.org/10.5194/bg-11-4493-2014

Huang, K., & Xia, J. (2019). High ecosystem stability of evergreen broadleaf forests under severe droughts. *Global Change Biology*, *25*(10), 3494-3503. https://doi.org/10.1111/gcb.14748

Huete, A., Didan, K., Miura, T., Rodriguez, E. P., Gao, X., & Ferreira, L. G. (2002). Overview of the radiometric and biophysical performance of the MODIS vegetation indices. *Remote Sensing of Environment*, *83*(1-2), 195-213. https://doi.org/10.1016/S0034-4257(02)00096-2

Hunter, J. D. (2007). Matplotlib: A 2D graphics environment. *Computing in Science & Engineering*, *9*(3), 90-95. https://doi.org/10.1109/MCSE.2007.55

Hutyra, L. R., Munger, J. W., Saleska, S. R., Gottlieb, E., Daube, B. C., Dunn, A. L., Amaral, D. F., De Camargo, P. B., & Wofsy, S. C. (2007). Seasonal controls on the exchange of carbon and water in an Amazonian rain forest. *Journal of Geophysical Research: Biogeosciences*, *112*, G3008. https://doi.org/10.1029/2006JG000365

Jeong, S.-J., Schimel, D., Frankenberg, C., Drewry, D. T., Fisher, J. B., Verma, M., Berry, J. A., Lee, J. E., & Joiner, J. (2017). Application of satellite solar-induced chlorophyll fluorescence to understanding large-scale variations in vegetation phenology and function over northern high latitude forests. *Remote Sensing of Environment*, *190*, 178-187. https://doi.org/10.1016/j.rse.2016.11.021

Jiao, W., Chang, Q., & Wang, L. (2019). The Sensitivity of Satellite Solar - Induced Chlorophyll Fluorescence to Meteorological Drought. *Earth's Future, 7*(5), 558-573. https://doi.org/10.1029/2018ef001087

Jing, W., Song, J., & Zhao, X. (2018). Validation of ECMWF multi-layer reanalysis soil moisture based on the OzNet hydrology network. *Water*, *10*(9), 1123. https://doi.org/10.3390/w10091123

Joiner, J., Guanter, L., Lindstrot, R., Voigt, M., Vasilkov, A. P., Middleton, E. M., Huemmrich, K. F., Yoshida, Y., & Frankenberg, C. (2013). Global monitoring of terrestrial chlorophyll fluorescence from moderate-spectral-resolution near-infrared satellite measurements: methodology, simulations, and application to GOME-2. *Atmospheric Measurement Techniques*, *6*(10), 2803-2823. https://doi.org/10.5194/amt-6-2803-2013

Jung, M., Reichstein, M., Margolis, H. A., Cescatti, A., Richardson, A. D., Arain, M. A., ... & Williams, C. (2011). Global patterns of land‐atmosphere fluxes of carbon dioxide, latent heat, and sensible heat derived from eddy covariance, satellite, and meteorological observations. *Journal of Geophysical Research: Biogeosciences, 116*, G00J07. https://doi.org/10.1029/2010JG001566

Jung, M., Reichstein, M., Schwalm, C. R., Huntingford, C., Sitch, S., Ahlstrom, A., Arneth, A., Camps-Valls, G., Ciais, P., Friedlingstein, P., Gans, F., Ichii, K., Jain, A. K., Kato, E., Papale, D., Poulter, B., Raduly, B., Rodenbeck, C., Tramontana, G., Viovy, N., Wang, Y. P., Weber, U., Zaehle, S., & Zeng, N. (2017). Compensatory water effects link yearly global land CO2 sink changes to temperature. *Nature*, *541*(7638), 516-520. https://doi.org/10.1038/nature20780

Jung, M., Schwalm, C., Migliavacca, M., Walther, S., Camps-Valls, G., Koirala, S., Anthoni, P., Besnard, S., Bodesheim, P., & Carvalhais, N. (2020). Scaling carbon fluxes from eddy covariance sites to globe: synthesis and evaluation of the FLUXCOM approach. *Biogeosciences*, *17*(5), 1343-1365. https://doi.org/10.5194/bg-17-1343-2020

Köhler, P., Guanter, L., & Joiner, J. (2015). A linear method for the retrieval of sun-induced chlorophyll fluorescence from GOME-2 and SCIAMACHY data. *Atmospheric Measurement Techniques*, *8*(6), 2589-2608. https://doi.org/10.5194/amt-8-2589-2015

Kraft, B., Jung, M., Körner, M., Mesa, C. R., Cortés, J., & Reichstein, M. (2019). Identifying dynamic memory effects on vegetation state using recurrent neural networks. *Frontiers in Big Data, 2*(31). https://doi.org/10.3389/fdata.2019.00031

Li, M., Wu, P., & Ma, Z. (2020). A comprehensive evaluation of soil moisture and soil temperature from third‐generation atmospheric and land reanalysis data sets. *International Journal of Climatology*, 1-23. https://doi.org/10.1002/joc.6549

Li, X., & Xiao, J. (2019). A Global, 0.05-Degree Product of Solar-Induced Chlorophyll Fluorescence Derived from OCO-2, MODIS, and Reanalysis Data. *Remote Sensing*, *11*(5). https://doi.org/10.3390/rs11050517

Li, X., & Xiao, J. (2020). Global climatic controls on interannual variability of ecosystem productivity: Similarities and differences inferred from solar-induced chlorophyll fluorescence and enhanced vegetation index. *Agricultural and Forest Meteorology*, 288-289. https://doi.org/10.1016/j.agrformet.2020.108018

Li, X., Xiao, J., He, B., Altaf Arain, M., Beringer, J., Desai, A. R., Emmel, C., Hollinger, D. Y., Krasnova, A., & Mammarella, I. (2018a). Solar‐induced chlorophyll fluorescence is strongly correlated with terrestrial photosynthesis for a wide variety of biomes: First global analysis based on OCO‐2 and flux tower observations. *Global Change Biology*, *24*(9), 3990-4008. https://doi.org/10.1111/gcb.14297

Li, X., Xiao, J., & He, B. (2018b). Higher absorbed solar radiation partly offset the negative effects of water stress on the photosynthesis of Amazon forests during the 2015 drought. *Environmental Research Letters*, *13*, 044005. https://doi.org/10.1088/1748-9326/aab0b1

Linscheid, N., Estupinan-Suarez, L. M., Brenning, A., Carvalhais, N., Cremer, F., Gans, F., Rammig, A., Reichstein, M., Sierra, C., & Mahecha, M. D. (2020). Towards a global understanding of vegetation-climate dynamics at multiple timescales. *Biogeosciences*, *17*(4), 945-962. https://doi.org/10.5194/bg-17-945-2020

Lundberg, S. M., & Lee, S. I. (2017). A unified approach to interpreting model predictions, Proc. Adv. Neural Inf. Process. Syst., pp. 4768-4777.

Madani, N., Kimball, J. S., Jones, L. A., Parazoo, N. C., & Guan, K. (2017). Global analysis of bioclimatic controls on ecosystem productivity using satellite observations of solar-induced chlorophyll fluorescence. *Remote Sensing*, *9*(6), 530. https://doi.org/10.3390/rs9060530

Martens, B., Gonzalez Miralles, D., Lievens, H., Van Der Schalie, R., De Jeu, R. A., Fernández-Prieto, D., Beck, H. E., Dorigo, W., & Verhoest, N. (2017). GLEAM v3: Satellite-based land evaporation and root-zone soil moisture. *Geoscientific Model Development*, *10*(5), 1903-1925. https://doi.org/10.5194/gmd-10-1903-2017

Matheny, A. M., Bohrer, G., Garrity, S. R., Morin, T. H., Howard, C. J., & Vogel, C. S. (2015). Observations of stem water storage in trees of opposing hydraulic strategies. *Ecosphere*, *6*(9), 1-13. https://doi.org/10.1890/ES15-00170.1

Migliavacca, M., Meroni, M., Manca, G., Matteucci, G., Montagnani, L., Grassi, G., ... & Seufert, G. (2009). Seasonal and interannual patterns of carbon and water fluxes of a poplar plantation under peculiar eco-climatic conditions. *Agricultural and Forest Meteorology, 149*(9), 1460-1476. https://doi.org/10.1016/j.agrformet.2009.04.003

Monteith, J. (1973). Principles of environmental physics. *Edward Arnold, London*.

Nemani, R. R., Keeling, C. D., Hashimoto, H., Jolly, W. M., Piper, S. C., Tucker, C. J., Myneni, R. B., & Running, S. W. (2003). Climate-driven increases in global terrestrial net primary production from 1982 to 1999. *Science*, *300*(5625), 1560-1563. https://doi.org/10.1126/science.1082750

Nippert, J. B., & Holdo, R. M. (2015). Challenging the maximum rooting depth paradigm in grasslands and savannas. *Functional Ecology*, *29*(6), 739-745. https://doi.org/10.1111/1365-2435.12390

Novick, K. A., Ficklin, D. L., Stoy, P. C., Williams, C. A., Bohrer, G., Oishi, A. C., Papuga, S. A., Blanken, P. D., Noormets, A., Sulman, B. N., Scott, R. L., Wang, L., & Phillips, R. P. (2016). The increasing importance of atmospheric demand for ecosystem water and carbon fluxes. *Nature Climate Change*, *6*(11), 1023-1027. https://doi.org/10.1038/nclimate3114

Oliphant, T. E. (2006). A guide to NumPy. *Trelgol Publishing USA*, Vol. 1.

O and Orth, Global soil moisture from in situ measurements using machine learning - SoMo.ml, Earth Syst. Sci. Data Discuss. (submitted), 2020

Orth, R., & Destouni, G. (2018). Drought reduces blue-water fluxes more strongly than green-water fluxes in Europe. *Nature Communications*, *9*, 3602. https://doi.org/10.1038/s41467-018-06013-7

Pearson, R. G., Phillips, S. J., Loranty, M. M., Beck, P. S., Damoulas, T., Knight, S. J., & Goetz, S. J. (2013). Shifts in Arctic vegetation and associated feedbacks under climate change. *Nature Climate Change*, *3*(7), 673-677. https://doi.org/10.1038/nclimate1858

Pedregosa, F., Varoquaux, G., Gramfort, A., Michel, V., Thirion, B., Grisel, O., Blondel, M., Prettenhofer, P., Weiss, R., & Dubourg, V. (2011). Scikit-learn: Machine learning in Python. *the Journal of Machine Learning Research*, *12*, 2825-2830.

Piao, S., Wang, X., Wang, K., Li, X., Bastos, A., Canadell, J. G., Ciais, P., Friedlingstein, P., & Sitch, S. (2020). Interannual variation of terrestrial carbon cycle: Issues and perspectives. *Global Change Biology*, *26*(1), 300-318. https://doi.org/10.1111/gcb.14884

Reichle, R. H., Koster, R. D., De Lannoy, G. J., Forman, B. A., Liu, Q., Mahanama, S. P., & Touré, A. (2011). Assessment and enhancement of MERRA land surface hydrology estimates. *Journal of climate*, *24*(24), 6322-6338. https://doi.org/10.1175/JCLI-D-10-05033.1

Sakschewski, B., Von Bloh, W., Boit, A., Poorter, L., Peña-Claros, M., Heinke, J., Joshi, J., & Thonicke, K. (2016). Resilience of Amazon forests emerges from plant trait diversity. *Nature Climate Change*, *6*(11), 1032-1036. https://doi.org/10.1038/nclimate3109

Schlaepfer, D. R., Bradford, J. B., Lauenroth, W. K., Munson, S. M., Tietjen, B., Hall, S. A., Wilson, S. D., Duniway, M. C., Jia, G., & Pyke, D. A. (2017). Climate change reduces extent of temperate drylands and intensifies drought in deep soils. *Nature Communications*, *8*, 14196. https://doi.org/10.1038/ncomms14196

Schulze, E.-D., Mooney, H. A., Sala, O., Jobbagy, E., Buchmann, N., Bauer, G., Canadell, J., Jackson, R., Loreti, J., & Oesterheld, M. (1996). Rooting depth, water availability, and vegetation cover along an aridity gradient in Patagonia. *Oecologia*, *108*(3), 503-511. https://doi.org/10.1007/BF00333727

Seddon, A. W., Macias-Fauria, M., Long, P. R., Benz, D., & Willis, K. J. (2016). Sensitivity of global terrestrial ecosystems to climate variability. *Nature*, *531*(7593), 229-232. https://doi.org/10.1038/nature16986

Seneviratne, S. I., Corti, T., Davin, E. L., Hirschi, M., Jaeger, E. B., Lehner, I., Orlowsky, B., & Teuling, A. J. (2010). Investigating soil moisture-climate interactions in a changing climate: A review. *Earth Science Reviews*, *99*(3-4), 125-161. https://doi.org/10.1016/j.earscirev.2010.02.004

Skipper, S. and Perktold, J. (2010). Sstatsmodels: Econometric and statistical modeling with python. Proceedings of the 9th Python in Science Conference.

Song, X. P., Hansen, M. C., Stehman, S. V., Potapov, P. V., Tyukavina, A., Vermote, E. F., & Townshend, J. R. (2018). Global land change from 1982 to 2016. *Nature*, *560*(7720), 639-643. https://doi.org/10.1038/s41586-018-0411-9

Stocker, B. D., Zscheischler, J., Keenan, T. F., Prentice, I. C., Peñuelas, J., & Seneviratne, S. I. (2018). Quantifying soil moisture impacts on light use efficiency across biomes. *New Phytologist*, *218*(4), 1430-1449. https://doi.org/10.1111/nph.15123

Stocker, B. D., Wang, H., Smith, N. G., Harrison, S. P., Keenan, T. F., Sandoval, D., Davis, T., & Prentice, I. C. (2020). P-model v1.0: an optimality-based light use efficiency model for simulating ecosystem gross primary production. *Geoscientific Model Development*, *13*(3), 1545-1581. https://doi.org/10.5194/gmd-13-1545-2020

Sun, Y., Fu, R., Dickinson, R., Joiner, J., Frankenberg, C., Gu, L., Xia, Y., & Fernando, N. (2015). Drought onset mechanisms revealed by satellite solar - induced chlorophyll fluorescence: Insights from two contrasting extreme events. *Journal of Geophysical Research: Biogeosciences*, *120*(11), 2427-2440. https://doi.org/10.1002/2015JG003150

Sundararajan, M., & Najmi, A. (2019). The many Shapley values for model explanation. *arXiv preprint, arXiv:1908.08474*

Tarek, M., Brissette, F. P., & Arsenault, R. (2020). Evaluation of the ERA5 reanalysis as a potential reference dataset for hydrological modelling over North America. *Hydrology and Earth System Sciences*, *24*(5), 2527-2544. https://doi.org/10.5194/hess-24-2527-2020

Tramontana, G., Jung, M., Schwalm, C. R., Ichii, K., Camps-Valls, G., Ráduly, B., Reichstein, M., Arain, M. A., Cescatti, A., Kiely, G., Merbold, L., Serrano-Ortiz, P., Sickert, S., Wolf, S., & Papale, D. (2016). Predicting carbon dioxide and energy fluxes across global FLUXNET sites with regression algorithms. *Biogeosciences*, *13*(14), 4291-4313. https://doi.org/10.5194/bg-13-4291-2016

Wagle, P., Zhang, Y., Jin, C., & Xiao, X. (2016). Comparison of solar - induced chlorophyll fluorescence, light - use efficiency, and process - based GPP models in maize. *Ecological Applications*, *26*(4), 1211-1222. https://doi.org/10.1890/15-1434

Walther, S., Duveiller, G., Jung, M., Guanter, L., Cescatti, A., & Camps - Valls, G. (2019). Satellite Observations of the Contrasting Response of Trees and Grasses to Variations in Water Availability. *Geophysical Research Letters*, *46*(3), 1429-1440. https://doi.org/10.1029/2018gl080535

Walther, S., Guanter, L., Heim, B., Jung, M., Duveiller, G., Wolanin, A., & Sachs, T. (2018). Assessing the dynamics of vegetation productivity in circumpolar regions with different satellite indicators of greenness and photosynthesis. *Biogeosciences*, *15*(20), 6221-6256. https://doi.org/10.5194/bg-15-6221-2018

Walther, S., Voigt, M., Thum, T., Gonsamo, A., Zhang, Y., Kohler, P., Jung, M., Varlagin, A., & Guanter, L. (2016). Satellite chlorophyll fluorescence measurements reveal large-scale

decoupling of photosynthesis and greenness dynamics in boreal evergreen forests. *Global Change Biology*, *22*(9), 2979-2996. https://doi.org/10.1111/gcb.13200

Wu, J., Albert, L. P., Lopes, A. P., Restrepo-Coupe, N., Hayek, M., Wiedemann, K. T., Guan, K., Stark, S. C., Christoffersen, B., & Prohaska, N. (2016). Leaf development and demography explain photosynthetic seasonality in Amazon evergreen forests. *Science*, *351*(6276), 972-976. https://doi.org/10.1126/science.aad5068

Lian, X., Piao, S., Li, L. Z., Li, Y., Huntingford, C., Ciais, P., Cescatti, A., Janssens, I.A., Peñuelas, J., Buermann, W., Chen, A., Myneni, R. B., Wang, X., Wang, Y., Yang, Y., Zeng, Z., Zhang, Y. & Mcvicar, T. R. (2020). Summer soil drying exacerbated by earlier spring greening of northern vegetation. *Science Advances*, *6*(1), eaax0255. https://doi.org/10.1126/sciadv.aax0255

Yan, H., Wang, S. Q., Huete, A., & Shugart, H. H. (2019). Effects of light component and water stress on photosynthesis of Amazon rainforests during the 2015/2016 El Niño drought. *Journal of Geophysical Research: Biogeosciences*, *124*(6), 1574-1590. https://doi.org/10.1029/2018JG004988

Yang, X., Tang, J., Mustard, J. F., Lee, J. E., Rossini, M., Joiner, J., Munger, J. W., Kornfeld, A., & Richardson, A. D. (2015). Solar - induced chlorophyll fluorescence that correlates with canopy photosynthesis on diurnal and seasonal scales in a temperate deciduous forest. *Geophysical Research Letters*, *42*(8), 2977-2987. https://doi.org/10.1002/2015GL063201

Zarco-Tejada, P. J., Morales, A., Testi, L., & Villalobos, F. J. (2013). Spatio-temporal patterns of chlorophyll fluorescence and physiological and structural indices acquired from hyperspectral imagery as compared with carbon fluxes measured with eddy covariance. *Remote Sensing of Environment*, *133*, 102-115. https://doi.org/10.1016/j.rse.2013.02.003

Zhang, Y., Peña-Arancibia, J. L., McVicar, T. R., Chiew, F. H., Vaze, J., Liu, C., Lu, X., Zheng, H., Wang, Y., & Liu, Y. Y. (2016). Multi-decadal trends in global terrestrial evapotranspiration and its components. *Scientific Reports*, 6, 19124. https://doi.org/10.1038/srep19124

Zuromski, L. M., Bowling, D. R., Köhler, P., Frankenberg, C., Goulden, M. L., Blanken, P. D., & Lin, J. C. (2018). Solar - induced fluorescence detects interannual variation in gross primary production of coniferous forests in the Western United States. *Geophysical Research Letters*, *45*(14), 7184-7193. https://doi.org/10.1029/2018GL077906

683 Zwillinger, D. and Kokoska, S. (2000). Standard Probability and Statistics Tables and Formulae.
684 *Florida: Chapman & Hall/CRC*.
685